

PROGRESS REPORT ON THE POPAE DESIGN STUDY\*

T.L. Collins, D.A. Edwards, J. Ingebretsen, D.E. Johnson,  
S. Ohnuma, A.G. Ruggiero, and L.C. Teng

Fermi National Accelerator Laboratory  
Batavia, Illinois

Summary

POPAE (Protons on Protons and Electrons) is a storage ring facility at the Fermilab on a scale suitable to permit the collision of 1000 GeV protons with 1000 GeV protons and with electrons of an energy compatible with that scale. In this paper, we summarize our work thus far on the lattice and layout of the proton storage rings. Though the 1000 GeV physical scale is maintained, the design is developed in a 400 GeV context. The proton rings form a racetrack, the two long straight sections of which are each about 1 km in length. Each long straight section contains a number of matched lattice insertions, as well as uncommitted space for additional development. Depending on the assumptions made concerning the beam-beam limit (as yet unknown experimentally), maximum luminosities are calculated to be in the range from  $10^{33}$  to  $10^{34} \text{cm}^{-2} \text{sec}^{-1}$ .

Introduction

POPAE was conceived at the Fermilab 1973 Aspen Summer Study as a storage ring facility on a scale suitable to permit the collision of 1000 GeV protons with 1000 GeV protons and with 20 GeV electrons. The luminosities were specified at  $10^{34} \text{cm}^{-2} \text{sec}^{-1}$  for proton-proton and  $10^{32} \text{cm}^{-2} \text{sec}^{-1}$  for electron-proton intersections. The general location of the facility was to the east of the present main accelerator, encircling the Fermilab Village. We have taken the Aspen plan as a starting point for our study, not from any preconception that it represents the optimum scale and site situation for POPAE, but rather from a feeling that its examination will represent an initial step in the development of a storage ring system design for the Fermilab.

However, we have found it necessary to modify the shape of the layout. At Aspen, a 240 meter length for each of the eight symmetrically disposed long straight sections was estimated to be sufficient to accommodate both the experiments and the machine components associated with the interaction region. Subsequent study indicated that 240 meters was insufficient, and in order to retain the 1000 GeV scale and general location of the rings, we have considered a racetrack form for POPAE, with approximately the same total straight section length as the Aspen version.

It has also been useful to adopt a design procedure in which we assume that we are designing proton storage rings to receive their injected beam from the present Fermilab synchrotron up to the energy at which it has demonstrated successful operation, namely, 400 GeV, and that the magnetic field of the bending magnets in the storage rings will be 18 kilogauss at this energy. These presumptions remove from present consideration a number of questions which can be debated endlessly and, most likely, profitlessly. Foremost among these are, first, the probability of existence of the Energy Doubler and its suitability as an injector for a storage ring, and second, the magnet-field levels that can be achieved by high quality,

economical, and reliable superconducting magnets. The physical scale of POPAE is unchanged by this design procedure, for the Aspen group had based their layout on 1000 GeV protons steered by 45 kilogauss dipoles.

Status

The layout of the present version of POPAE on the Fermilab site is sketched in Figure 1. The two long straight sections are unequal in length as a result of the east-west asymmetry of the system with regard to injection. They are parallel to each other and parallel to the eastern boundary of the site.

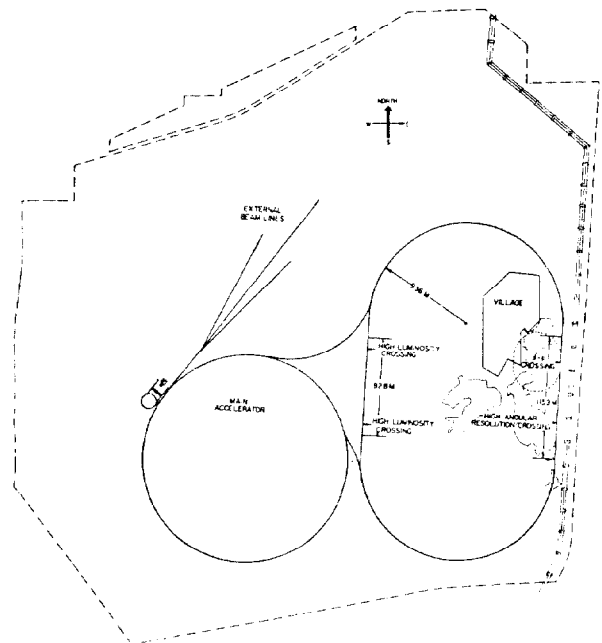


Fig. 1. Layout of POPAE on the Fermilab site. The large "racetrack" represents an enclosure containing the two proton storage rings. Of the two alternatives considered for the electron ring, one - the 20 GeV case - would share the same enclosure as the proton rings. The second possibility - a 10 GeV electron ring - is shown as the small dashed oval.

Insofar as the machine optics are concerned, several interaction regions can be placed in each long straight section. However, only two regions for experiments are shown on each side. There are several reasons for this. We have included only those interaction region types that have thus far been sufficiently well defined. It is likely that additional insertion requirements will arise as time goes on. Second, any modern storage ring design, regardless of its apparent symmetry, will be nevertheless a periodic focusing system of one-fold rotational symmetry when in operation, and at least

\*Work supported by the U.S. Energy Research and Development Administration.

during the initial phases of its running, will need an allocation of adequate space for beam-optics adjusting systems which are needed for the compensation of the consequences of low periodicity. Finally, there is the thought that a facility of this magnitude should be planned with the potential for future development. Of course, this last argument must ultimately be tempered by the realities of costs.

The injection lines are shown proceeding from two successive long straight sections of the main accelerator. The mean radius of the curved portions of these lines is smaller than that in the storage rings and is based on a 90% packing factor; however, the 18 kilo-gauss limitation has been observed here as well.

The remainder of this paper describes the lattice of the proton storage rings and related topics. The electron ring is not treated in this report. Unless otherwise indicated, the current in each proton ring is taken to be 10A with a transverse emittance,  $\epsilon \cong 6\pi\sigma^2/\beta$ , of  $\pi/40$  mm-mrad in either plane at 400 GeV. A more detailed discussion of chromatic aberration effects in our one-fold periodic structure will be found in paper K-15 at this conference.<sup>1</sup>

### General Description of the Lattice

The proton storage ring lattice has been developed on the basis of the following specifications in addition to those stated in the introduction:

- The storage rings are located one above the other. The beams are brought together in the vertical plane to collide.

- The separated function normal cell is of the FODO structure, and the most advantageous phase advance per cell for beam manipulation is  $90^\circ$ . The normal cell length is taken to be 60 m, and four bending magnets, each about 6 m in length, are situated between successive quadrupoles.

- To facilitate the design of matched insertions, all pairs of corresponding quadrupoles in the two rings are assumed to have opposite focusing actions on the two beams, hence the same gradient polarity. The reasons for this choice are outlined in the following section entitled Insertions.

- The lattice modifications to accommodate injection will be identical in both rings and the injection points will be symmetrically located to the north and south of the mid-point of the west long straight section.

- The bending elements in the north and south arcs will be distributed so as to bring the momentum dispersion function to zero or nearly so throughout the long straight sections.

For injection, we follow the method outlined in the 1968 Fermilab storage ring report,<sup>2</sup> which utilizes full aperture kickers to produce a transient localized orbit distortion positioning the injection beam orbit on the "other" side of a septum. It is desirable to modify the momentum dispersion function,  $\eta$ , in the injection area so that  $\eta$  will be large at the septum position. An arrangement which provides space for the injection elements and accomplishes the  $\eta$  modification is obtained by the omission of dipole magnets from four half-cells. An "empty" half-cell

for the injection septum is followed two normal cells downstream ( $180^\circ$  in betatron oscillation phase) by a second empty half-cell to localize the perturbation in  $\eta$ . Two empty half-cells  $720^\circ$  apart in betatron phase and located equidistantly upstream and downstream of the septum accommodate the full aperture kickers and increase  $\eta$  at the injection points by nearly a factor of two. Their  $720^\circ$  separation insures that that perturbation in  $\eta$  will be limited to the region between the kicker positions. The placement of the injection portion of the lattice in the north and south arcs can be adjusted in half-cell increments to optimize the location of the injection points.

Dispersion reduction for the long straight sections can also be effected by omission of dipoles from the normal lattice. For  $90^\circ$  cells, one may readily show that an empty-normal-empty sequence of half cells will bring  $\eta$  to zero at the end with the same  $\eta' \cong d\eta/dz$  regardless of the sign of the quadrupoles. The slope  $\eta'$  may then be brought to zero by the placement of two normal-cell dipoles at the last quadrupole in the sequence. The normal cell, as discussed below, does not have its bending magnets located symmetrically about the middle of a half cell. Nor can the equivalent of two bending magnets be superimposed upon a quadrupole. So slight modification of the foregoing arrangement would be necessary to set  $\eta$  precisely to zero. We have assumed that minor dispersion adjustments will be performed near the interaction regions and have been satisfied with the removal of the bulk of the dispersion at the ends of the straight sections by this arrangement.

The injection point is located at an angle of  $15.6^\circ$  with respect to the direction of the long straight section. A final adjustment of the long straight section lengths has been made so that the path length of the injected orbit corresponds to a harmonic number of 1507 at the frequency of the main accelerator rf system. The resulting lattice is summarized schematically in Figure 2.

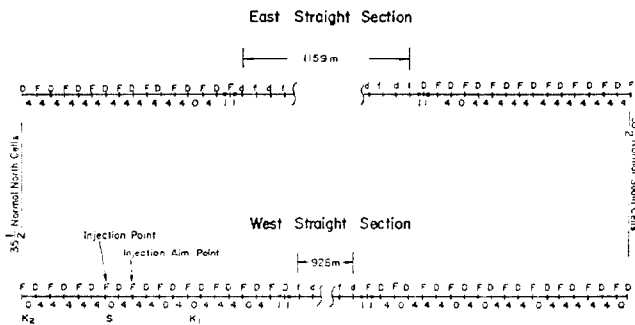


Fig. 2. Schematic of lattice for Beam 1 (clockwise). Lattice for Beam 2 is obtained by interchange of F, D designations, and by north-south reflection of the injection sequence. Quadrupole focusing character is referred to horizontal plane. Numerals below half-cell intervals indicate number of dipoles in half-cell.

### Insertions

Each long straight section consists of a sequence of several matched insertions, as shown in Figure 3. A modular approach<sup>3</sup> has been followed in the sense that a standard set of matching conditions has been used at either end of each insertion. Namely,  $\eta$  and  $\eta'$  are taken to be zero, while the amplitude functions join

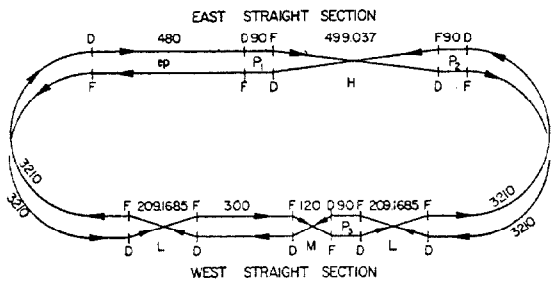


Fig. 3. Composition of long straight sections. Insertions are: L - high luminosity, H - high angular resolution, P - phase adjusting, M - non-colliding crossing. All distances are in meters.

properly to those in a normal cell. The design of the insertions has been carried out using the computer programs MAGIC<sup>4</sup> and TRANSPORT.<sup>5</sup>

We assume all crossings of the two beams to be in the vertical plane and all quadrupoles are paired with one directly above the other and of equal strength. There are then two alternative arrangements: each pair of quadrupoles could have either the same focusing action on the two beams (denoted by F/F) or the opposite focusing actions (F/D). In the focusing sequence in each beam, there are also two alternatives: the quadrupole focusing actions can have reflection symmetry about the insertion midpoint (symmetric) or reflection symmetry with change of sign (antisymmetric). In an antisymmetric insertion, the beam optics in the horizontal and vertical planes are midpoint reflections of each other, hence, the phase advances of betatron oscillations in the two planes are identical. For this reason, we consider antisymmetric insertions generally more desirable, although the different optics in the two planes obtainable in a symmetric insertion can be advantageous in special cases. The F/F arrangement applied to an antisymmetric insertion does not necessarily yield a geometry in the vertical plane for the two beams which has reflection symmetry about the midpoint, thereby making the design of such a crossing insertion more complicated. For the present design, we have adopted the F/D arrangement as being simpler and more symmetric. Additionally, the F/D case permits the use of quadrupoles common to both beams. To exploit the simplicity thus acquired, we have extended this arrangement to the entire rings as stated above.

#### High Luminosity Insertion

The requirements for this insertion are that (a) the beams be focused to the smallest width reasonably possible at the (vertical) crossing to achieve high luminosity, (b) the length of the luminous region be reasonably short and well defined, (c) space adequate for experimental equipment be allowed between the beam transport elements on either side of the crossing point, and (d) space be available next to the outgoing beams for detection of forward secondaries.

Condition (a) implies that the horizontal dispersion vanish at the crossing, and the horizontal amplitude function,  $\beta_H^*$  be reduced insofar as is practicable there. Conditions (a) and (b) imply that the crossing angle be small, that the vertical dispersion vanish at the crossing point, and that  $\beta_V^*$  be small.

The desire for small  $\beta_H^*$  and  $\beta_V^*$  runs counter to condition (c), for the smaller the value of  $\beta$  at the crossing, the larger its value elsewhere in the

insertion. We have chosen not to allow the amplitude function to exceed by more than an order of magnitude its value in a normal cell. Further, we have assumed that the free length on either side of the crossing point should not be less than 20 m. The lower limit for either  $\beta_H^*$  or  $\beta_V^*$  is then about 1 m. With these values of  $\beta^*$ , a crossing angle,  $\alpha$ , of 1 mrad will then result in a reduction of the luminosity per unit length to below one part in ten thousand at a distance of 50 cm on either side of the crossing point for beams of the emittance provided by the main accelerator at 400 GeV.

With currents of 10 amperes in each beam, the luminosity at such a crossing would be  $10^{34} \text{ cm}^{-2} \text{ sec}^{-1}$ . The beam-beam tune shift under these conditions exceeds the canonical figure of 0.005. Since we are dealing with Gaussian beams with  $\beta_H^* = \beta_V^*$  at the crossing point, we may use the results of Keil, Pellegrini, and Sessler<sup>6</sup> to calculate the beam-beam tune shift, and find a short range contribution of 0.01 which is enhanced by 50% when the long range effect is taken into account. However, the luminosity indicated above is rather high. The present design provides entirely adequate luminosities at a tune shift of 0.005 and allows improvements should the true limit prove to be higher.

Because of the small crossing angle, to keep the long range tune shift from becoming excessively large, the beams must be separated at both ends of the crossing region by strong, large aperture dipoles. For the F/D arrangement, these dipoles can be located next to the quadrupole pairs either on the inboard or outboard sides. To investigate forward secondaries, one must detect particles which pass through the apertures of both the dipole and the quadrupole pair. If the dipoles are on the inboard side, they will sweep charged secondaries onto the yokes of the quadrupoles. But if the quadrupoles are on the outboard side, most of the charged particles can pass through the quadrupole apertures and be swept out of the beam by the following large aperture dipoles into the detectors. This implies that the quadrupole pairs be used commonly by both beams. We have adopted this design. Furthermore, in the beam branches leading away from the crossing point, the common dipole is followed by a 25 m drift space to facilitate placement of detectors. The high luminosity insertion conforming to the specifications above is represented below.

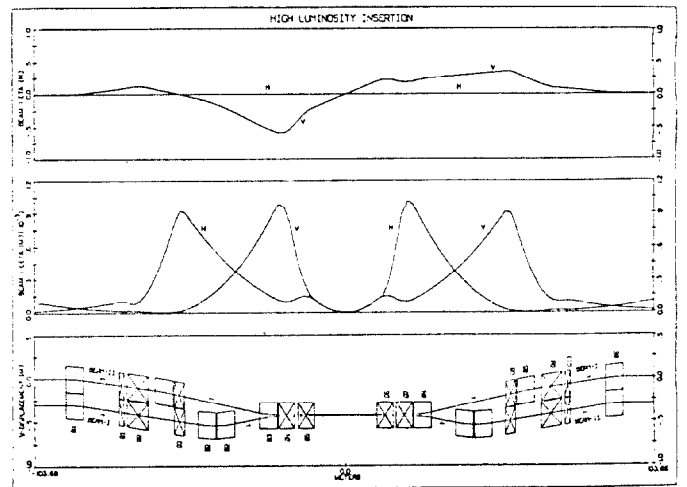


Fig. 4. Lattice elements and orbit parameters for high luminosity insertion.  $\beta_H^* = \beta_V^* = 1$  meter and  $\alpha = 1$  mrad.

## High Angular Resolution Insertion

The parameters of this insertion have been selected to make feasible measurements on p-p scattering at angles where the nuclear and coulomb amplitudes are comparable. At 400 GeV, this situation corresponds to a scattering angle of 0.1 mrad, and the angular width of the beam must be well below this figure; we have chosen  $\beta^* = 500$  m, yielding an angular beam width of 0.014 mrad. For the same reason,  $\eta'$  has been set to zero at the crossing. Detectors for the small angle process will be located next to the beam downstream in the outgoing branches and the scattered particles will pass through a number of insertion elements to reach them. In order to achieve parallel-to-point optics from the crossing to the detectors, we require  $90^\circ$  phase advance of betatron oscillations between these points, and that  $\eta$  vanish at the detectors. Further,  $\beta$  must be large enough at the detectors so as not to place unrealistic demands on their spatial resolution. We have taken  $\beta = 20$  m at these points which gives a separation of 1.4 mm for two particles differing in direction by 0.014 mrad at the crossing. The crossing angle is chosen to be 10 mrad, reflecting a compromise between the growth of the beam-beam tune shift with decreasing crossing angle, and the lower luminosity and larger total vertical bending associated with bigger crossing angles. The distribution of vertical bending magnets has been adjusted to improve access to the neighborhood of the outgoing beams for the study of other small angle processes. The resulting insertion is illustrated in Figure 5.

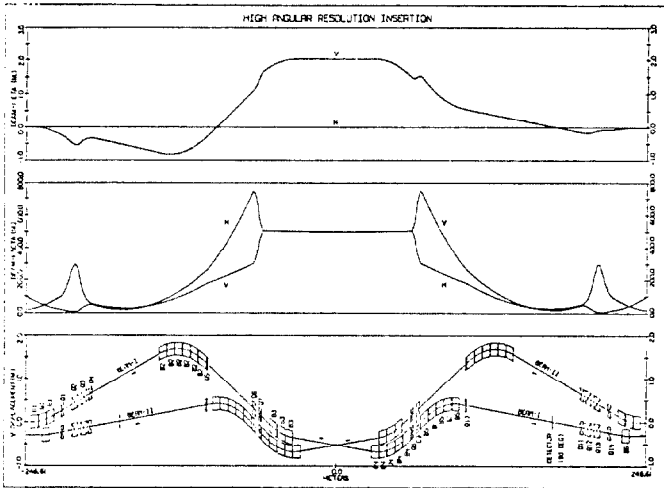


Fig. 5. Lattice elements and orbit parameters for high angular resolution insertion.

$$\beta_H^* = \beta_V^* = 500 \text{ m and } \alpha = 10 \text{ mrad.}$$

At 10A per beam, the luminosity would be  $5 \times 10^{31} \text{ cm}^{-2} \text{ sec}^{-1}$ , far greater than that needed for the measurement of scattering in the nuclear-coulomb interference region and sufficient to yield a rate of  $\sim 4$  counts per minute in  $\Delta|t|$  bins of  $0.05 (\text{GeV}/c)^2$  at  $t \sim 1 (\text{GeV}/c)^2$ . At this peak luminosity, the linear beam-beam tune shift would be 0.022, comparable with that in the high luminosity insertion.

### Phase Adjusting Insertion

The phase adjusting insertion is a sequence of eight quadrupoles occupying 90 m of straight section - in effect, replacing four quadrupoles of the normal lattice. They are powered separately from the normal lattice quadrupoles, and by varying their excitation,

the betatron phase advance through the insertion can be adjusted over a range of  $100^\circ$  - the same in both planes.

In each ring, one of these insertions is interposed between each pair of proton-proton interaction regions. They play a number of roles in our design procedure. First, they provide a means of tune adjustment without changing the normal cell phase. Second, as described elsewhere,<sup>1</sup> certain effects of chromatic aberration may be decoupled from one interaction region to another. Third, they facilitate the study of the variation of beam parameters as the intersecting insertions are tuned to conditions other than those for which they were designed. At a later stage in our work, it may prove feasible to eliminate one or more of this type of insertion; however, for the present, the phase adjusting insertion introduces a valuable degree of flexibility into the lattice.

### The Non-Colliding Crossing Insertion

With three colliding intersections, there must be (at least) one more place where the beams interchange their relative positions in the vertical plane. In order that the injection geometry be the same for both rings, we have placed this additional crossing in the west long straight section where it occupies the space of two normal cells. This insertion is of the symmetric type. Arranging the crossing to occur at the midpoint of a quadrupole in the normal sequence maximizes the drift on either side so that the beams are more readily separated before encountering the next lattice elements.

### The Normal Cell

The normal cell resembles that of the main accelerator - a straight-forward FODO cell with a length of 60 m. Each half cell contains four 5.9 m dipoles, a quadrupole of length 1.8 m, four 0.4 m intermagnet gaps and a 3 m straight section, which is placed on the east side of the quadrupole in both the north and south arcs of the rings (this arrangement enables the injection elements to be situated identically in the two rings). The straight section is intended to accommodate vacuum equipment, correction elements, and beam monitoring devices.

Though magnet design is not part of the present phase of our study, a few remarks are in order here to indicate the sort of magnets that we have in mind at the moment. The 18 kG dipoles are visualized as superconducting "window-frame" magnets with an aperture that is approximately square. They may be characterized as a low field version of the magnets developed by Danby and collaborators at BNL.<sup>7</sup> Corresponding magnets of the two rings are in a common cryostat, and we have taken the vertical separation between the two proton beams to be 30 cm. By extension of the roughly square steel geometry, the quadrupoles are envisioned to be of the Panofsky-Hand configuration.

As implied by the small intermagnet gaps, we have assumed that a cold bore vacuum system will prove to be feasible and that pumping stations will not be required between each pair of magnets. There is no reason to believe that the pressure requirements will be any less stringent than those in the ISR. Thus at liquid helium temperatures, the pressure should not exceed some  $5 \times 10^{-13}$  Torr. Despite the pumping speed offered by cryogenic surfaces, the high desorption coefficients of helium and hydrogen adsorbed in sufficient quantities suggest that surface cleanliness will remain a consideration. The diameter of our circular

beam pipe is taken to be 7.6 cm (3 inches) primarily for reasons of vacuum stability, for Benvenuti has concluded<sup>8</sup> that based on current knowledge of surface phenomena, a vacuum chamber of this size would be adequate for maintenance of pressure stability in the presence of a 10A circulating current.

The injection and stacking procedure outlined below implies the need for a good field region some 5 cm in horizontal extent. If the steel and coils forming the inner boundaries of the magnet aperture describe a square 10 cm on a side, a somewhat larger region of good field quality can likely be achieved to make allowance for orbit distortions, beam manipulation, and less rapid degradation of luminosity at lower energy.

The use of a circular beam pipe, made of a material having a high conductivity at low temperature, such as aluminum, has the consequence of removing certain high current phenomena from contention as aperture determining factors.

### Injection and Stacking

We conclude with a brief discussion of injection and stacking. Momentum stacking has proved to be very successful at the ISR and we follow the same procedure for POPAE. The  $5 \times 10^{13}$  protons per pulse intensity goal for the Fermilab accelerator is based on a multi-turn mode of injection into the booster synchrotron; for injection into storage rings, the low-emittance single turn mode is preferable and has yielded  $10^{13}$  protons per main accelerator cycle. The emittance figures used earlier in this paper are associated with the single turn method.

A 10A beam in one of the storage rings requires 180 injector pulses if there is no loss during transfer. Assuming that during stacking, the momentum phase-space density is diluted to 75%, the momentum width of the stack would be 240 times the momentum width of a single pulse. Our longitudinal emittance per rf bunch of 0.1 eV-sec translates into a fractional momentum spread at 400 GeV of  $1.3 \times 10^{-5}$  when debunched. The total momentum width of the stack will then be 0.3%. At the injection point, where  $n$  has been increased to about 4.5 m, this fractional momentum width becomes a physical width of 17 mm at 400 GeV.

If we assume that 10 mm should be allowed for space to permit a septum to be interposed between the stack and the "inner" edge of the injected beam and that stacking "at the top" is to be used, each accelerated pulse will be decelerated by about 2.4 GeV.

Selecting a compromise between shorter deceleration times on the one hand and high stacking efficiency and lower cavity voltage on the other, a time of 10 seconds is found for the stacking of each injected pulse. This is reasonable both for injector performance and overall injection time.

Tailoring to the bunch shape should be done in the main accelerator prior to transfer where the inevitable losses are less critical. It is difficult to insure proper phasing between the main accelerator and the storage rings because of the large distance between them. The injected pulse itself can be used to establish the phasing. The 7 usec interval between the end of the injected pulse and the beginning of the second passage of the beam through the rf system allows ample time for adjustment of rf system phase.

### References

- <sup>1</sup>D.A. Edwards, S. Ohnuma, L.C. Teng, "Compensation of Chromatic Aberration in a Single Period Lattice," Paper K-15, this conference.
- <sup>2</sup>"Proton-Proton Colliding-Beam Storage Rings for the National Accelerator Laboratory," 1968 Design Study, edited by L.C. Teng.
- <sup>3</sup>W.W. Lee and L.C. Teng, "Insertions for Colliding-Beam Storage Rings," Proceedings of the IXth International Conference on High Energy Particle Accelerators, SLAC 1974, page 599.
- <sup>4</sup>M.J. Lee, W.W. Lee and L.C. Teng, "Magnet Insertion Code (MAGIC)," 1973 PEP Summer Study.
- <sup>5</sup>K.L. Brown, R.F. Rothacker, D.C. Carey, and Ch. Iselin, "TRANSPORT - A Computer Program for Designing Charged Particle Beam Transport Systems," NAL-91, or SLAC 91, or CERN 73-16, March 1974.
- <sup>6</sup>E. Keil, C. Pellegrini, and A.M. Sessler, "Tune Shifts for Particle Beams Crossing at Small Angles in the Low- $\beta$  Section of a Storage Ring," CERN Report CERN/ISR-TH/73-44, September 1973.
- <sup>7</sup>See, for example, J. Allinger, G. Danby, B. DeVito, S. Hsieh, J. Jackson, A. Prodell, "Studies of Performance and Field Reproducibility of a Precision 40 kG Superconducting Dipole Magnet," IEEE Transactions on Nuclear Science, Volume NS-20, 678 (1973).
- <sup>8</sup>C. Benvenuti, "Vacuum System for Proton Storage Rings Equipped with Superconducting Magnets," FERMILAB-74/109, December 1974.